Monotone embedded discrete fractures method for flows in porous media

Kirill D. Nikitin * Ruslan M. Yanbarisov

March 5, 2019

1 Embedded Discrete Fracture Method

The main advantage of EDFM is its ability to account accurately fractures using additional degrees of freedom on meshes not fitted to fractures. The method has obtained close attention in the last few years [5, 4, 6, 7]).

In our work, fractures are assumed to be planar 3D regions with fixed geometry and thickness. Cell-fracture intersection data can be obtained using general triangle-triangle intersection algorithms. Since the fracture geometry is fixed, it is sufficient to compute this data and transmissibility indices at the model setup stage.

We consider long fractures with lengths $L_f \gg h$ (h is the mesh size) since fractures of smaller length can be accounted by modifying local permeability of mesh cells. The fracture width w_f is assumed to be less than h, so one can not resolve fractures on reservoir mesh.

The EDFM for the diffusion model is formulated as follows. We introduce two separate domains for fracture and medium and p^f, p^m unknowns defined in fracture and medium domains, respectively. Let $\mathbf{q} = -\mathbb{K}\nabla p$ denote the diffusion flux, then $\mathbf{q}^f = -\mathbb{K}^f \nabla p^f, \mathbf{q}^m = -\mathbb{K}^m \nabla p^m$.

1. Using a monotone FV method we discretize equations for the porous media:
$$\operatorname{div} \mathbf{q}^m = g^m + \sum_i q_{F_i,m}, \tag{1}$$

2. Using the linear TPFA-FV method we discretize equations for the fractures:
$$\operatorname{div} \mathbf{q}^f = g^f - \sum_i q_{F_i,m}, \tag{2}$$

where $q_{F_i,m}$ is the fracture-matrix flow term from fracture F_i to the medium.

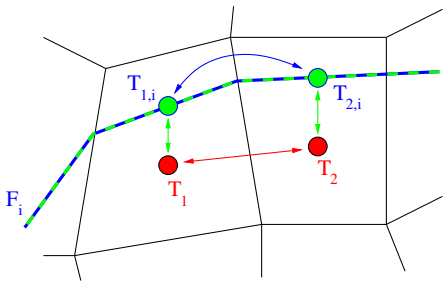

Figure 1: Darcy fluxes for a fracture in porous media: cell-to-cell (red), cell-to-fracture (green) and intra-fracture (blue) exchanges.

For the sake of consistency, when a fracture intersects the boundary, the unknown p^f should satisfy the boundary condition for unknowns in porous media.

Application of the finite volume method for the coupled fracture-media system (1)-(2) requires three types of fluxes (see Figure 1): cell-to-cell, cell-to-fracture and intra-fracture exchanges. For the case of several intersecting fractures we also add fracture-to-fracture fluxes.

For a given polyhedral mesh $\mathcal{T}$, the EDFM for the Darcy fluxes in the cell T with n_T fractures F_i can be formulated as follows:

$$\sum_{f\in\partial T} \mathbf{q}_f\cdot\mathbf{n}_f - \sum_{i=1,\dots,n_T} q_{F_i,T} = \int_T g d\mathbf{x}, \tag{3}$$

$$\sum_{f_j\in\partial T_i} q_{F_i,f_j} + \sum_{j=1,\dots,n_T} q_{F_{i,j},T} + q_{F_i,T} = \int_{T_i} g d\mathbf{x}, \qquad i=1,\dots,n_T, \tag{4}$$

where $\mathbf{q}_f\cdot\mathbf{n}_f$ is the cell-to-cell diffusive flux between the cell T and its neighbor through the face f and $q_{F_i,T}$ is the cell-to-fracture flux from cell T to fracture F_i. Equation (4) is written for each virtual fracture cell $T_i = F_i\cap T$ with intra-fracture fluxes q_{F_i,f_j} through virtual faces f_j of T_i. Also equation (4) accounts the fracture-to-fracture flux $q_{F_{i,j},T_j}$ between the fracture cell T_i and other fracture cells $T_j = F_j\cap T$. It should be noted that

$$q_{F_{i,j},T} = -q_{F_{j,i},T}.$$

1.1 Cell-to-cell flux

For the monotone EDFM we use the nonlinear FV schemes for the cell-to-cell fluxes in (3): nonlinear monotone TPFA [3] or nonlinear MPFA satisfying the discrete maximum principle (DMP) [2, 8]. For the sake of comparison we

*Marchuk Institute of Numerical Mathematics, Russian Academy of Sciences, Moscow; nikitin.kira@gmail.com

will also use two conventional linear schemes: linear TPFA and linear MPFA (O-scheme) [1].

The nonlinear schemes are constructed as follows. For each cell-face pair we need to find a triplet (see Figure 2 for a 2D example), a set of three vectors $\mathbf{t}_*$ such that for the co-normal vector $\boldsymbol{\ell}_f = \mathbb{K} \cdot \mathbf{n}_f$ we have

$$\boldsymbol{\ell}_f = \alpha\ \mathbf{t}_1 + \beta\ \mathbf{t}_2 + \gamma\ \mathbf{t}_3, \tag{5}$$

where coefficients α, β and γ are non-negative.

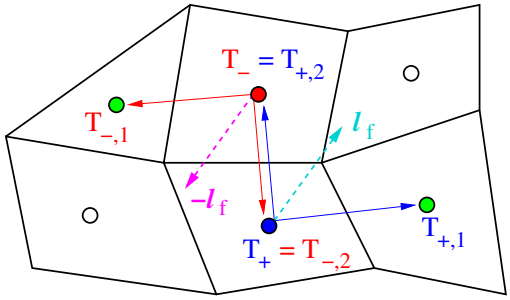

Figure 2: Two representations of co-normal vector $\boldsymbol{\ell}_f = \mathbb{K} \cdot \mathbf{n}_f$ (2D example).

Since the flux normal component is in fact the directional derivative along the co-normal vector $\boldsymbol{\ell}_f$, it can also be represented as the sum of three derivatives along $\mathbf{t}_*$ which are approximated by central differences:

$$q_+ = \alpha'_+\ (p_+ - p_{+,1}) + \beta'_+\ (p_+ - p_{+,2}) + \gamma'_+\ (p_+ - p_{+,3}), \tag{6}$$

where for cell T_+ coefficients $\alpha'_+, \beta'_+, \gamma'_+$ are normalized by coefficients $|\mathbf{t}_{+,i}|/|\boldsymbol{\ell}_f|$ from (5).

For the opposite co-normal vector $-\boldsymbol{\ell}_f$ we have the similar representation with non-negative coefficients:

$$q_- = \alpha'_-\ (p_- - p_{-,1}) + \beta'_-\ (p_- - p_{-,2}) + \gamma'_-\ (p_- - p_{-,3}). \tag{7}$$

Now we can take a linear combination of (6) and (7) with non-negative coefficients μ_+ and μ_-:

$$\mathbf{q}_f \cdot \mathbf{n}_f = \mu_+ q_+ + \mu_-(-q_-). \tag{8}$$

Flux approximation requires the linear combination of μ_+, μ_- to be convex:

$$\mu_+ + \mu_- = 1. \tag{9}$$

The second equation of the coefficients $\mu_\pm$ defines the features of the resulting scheme:

- To construct the *two-point* nonlinear monotone discretization, we set to zero the contributions to (8) of all the cells except for T_+, T_-:

  $$-\mu_+ d_+ + \mu_- d_- = 0, \tag{10}$$

  where $d_\pm = \alpha'_\pm\ p_{\pm,1} + \beta'_-\ p_{\pm,2} + \gamma'_-\ p_{\pm,3}$;

- To construct the *multi-point* nonlinear discretization satisfying the DMP, we set equal two representations of the flux:

$$\mu_+ q_+ = -\mu_- q_-. \tag{11}$$

The solution of the equations (9)-(11) is considered in detail in [3, 2].

1.2 Cell-to-fracture flux

For each grid block T and fracture F_i, the diffusive flux between the fracture and the matrix is

$$q_{F_i,T} = \lambda_{F_i,T}(p_T - p^f_{T,i}). \tag{12}$$

In order to compute transmissibility $\lambda_{F_i,T}$, we use the transport index approach suggested in [5]. The transmissibility index depends on grid geometry and media physical properties which are known during the simulation. One possible approach for its calculation is to use the half of harmonic average of the fracture λ_{F_i} and medium λ_T transmissibilities:

$$\lambda_{F_i,T} = \frac{\lambda_{F_i}\lambda_T}{\lambda_{F_i} + \lambda_T},$$

where

$$\lambda_T = \frac{2A}{< d >_{T,F_i}} \left(\mathbf{n} \cdot \mathbb{K}_T \mathbf{n}\right), \quad \lambda_{F_i} = \frac{2A}{w_i} k_i^f.$$

Here k_i^f is the isotropic permeability within fracture F_i, A is the fracture surface area inside a grid block T, $\mathbf{n}$ is the normal vector to fracture inside T and $< d >_{T,F_i}$ is the averaged normal distance from the fracture to the cell [5]:

$$< d >_{T,F_i} = \frac{\int_T x_{F_i}(\mathbf{x}')d\mathbf{x}'}{|T|},$$

where x_{F_i} is the distance from the fracture and $|T|$ is the cell volume.

1.3 Intra-fracture flux

For each fracture F_i crossing grid blocks $T_{1,i}$ and $T_{2,i}$ with common face f we use a 2D FV scheme for the fracture surface mesh with virtual cells belonging to $T_{1,i}$ and $T_{2,i}$. The FV scheme uses collocation of degrees of freedom at the centers of the virtual cells.

The Darcy flux between fracture cells $T_{1,i}$ and $T_{2,i}$ is

$$q_{F_i,f} = \lambda_{F_i,f}(p^f_{T_{2,i}} - p^f_{T_{1,i}}), \tag{13}$$

where the transmissibility in the isotropic media of the fracture is

$$\lambda_{F_i,f} = \frac{k_i^f \, s \, w_i}{a_2 + a_1}, \tag{14}$$

Here w_i is the fracture width, s is the length of the fracture intersection with the face f between cells $T_{1,i}$ and $T_{2,i}$, and a_1, a_2 are the distances from virtual fracture cell centroids to the face between $T_{1,i}$ and $T_{2,i}$ (see Figure 3).

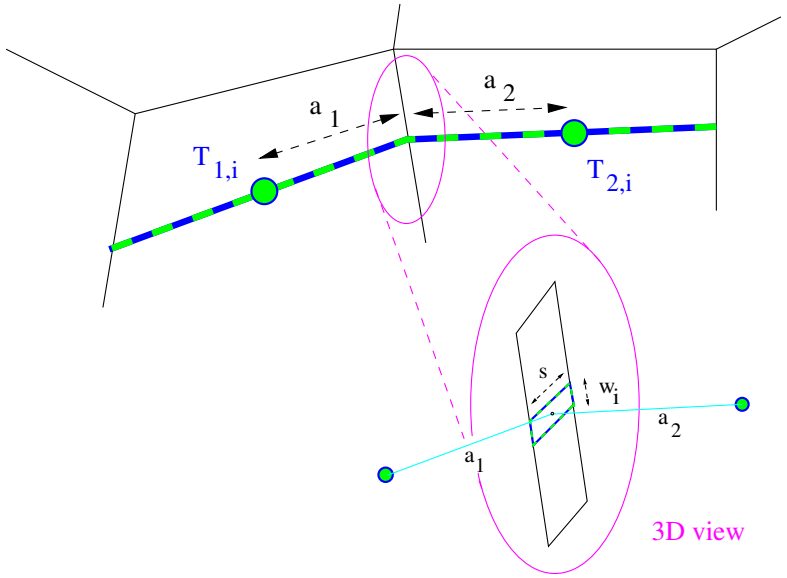

Figure 3: Flux approximation in fracture.

1.4 Fracture-to-fracture flux

Intersection of fractures F_i and F_j is a segment which can cross several mesh cells. Within each cell T, flow between intersecting fractures can be computed as follows [6]:

$$q_{F_{i,j},T} = \lambda_{F_{i,j},T}(p_i^f - p_j^f) \tag{15}$$

with

$$\lambda_{F_{i,j},T} = \frac{\lambda_{F_i}\lambda_{F_j}}{\lambda_{F_i} + \lambda_{F_j}}, \qquad \lambda_{F_i} = \frac{k_i^f w_i s}{a}.$$

Here w_i is the width of fracture F_i, s is the segment intersection length, a is the averaged normal distance from the center of the fracture subsegments inside gridblock T (located at each side of the intersection line) to the intersection line (see Figure 4).

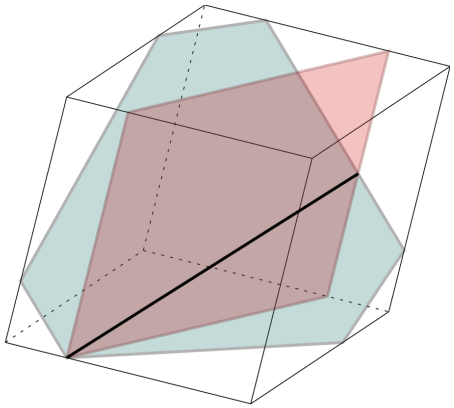

Figure 4: Two intersecting fractures inside grid block require non-neighbouring connection between fracture control volumes.

2 Analysis of the monotone EDFM

The following statement may be formulated for the diffusion equation (the single-phase pressure equation):

Theorem 2.1. *Let extremum-preserving nonlinear MPFA scheme is used for inter-cell Darcy flux discretization. Then the monotone EDFM from sections 1.1–1.4 with Darcy fluxes* (3)–(4) *is also extremum-preserving.*

Proof. *It was shown in [2] that that if the nonlinear algebraic system generated by the nonlinear MPFA is solved by the Picard method, then the resulting linear system is an M-matrix* $\mathbf{M}$*, that has the diagonal dominance in rows. If the nonlinear method converges, then the DMP holds for each iterate and the converged solution.*

Addition of the fracture degrees of freedom and the cell-to-fracture, intra-fracture and fracture-matrix fluxes is performed by assembling of 2×2 *matrices* $\mathbf{M}_{F_i,T}$, $\mathbf{M}_{F_i,f}$ *and* $\mathbf{M}_{F_{i,j},T}$*:*

$$\mathbf{M}_{F_i,T} = \begin{pmatrix} \lambda_{F_i,T} & -\lambda_{F_i,T} \\ -\lambda_{F_i,T} & \lambda_{F_i,T} \end{pmatrix}, \qquad \mathbf{M}_{F_i,f} = \begin{pmatrix} \lambda_{F_i,f} & -\lambda_{F_i,f} \\ -\lambda_{F_i,f} & \lambda_{F_i,f} \end{pmatrix}, \qquad \mathbf{M}_{F_{i,j},T} = \begin{pmatrix} \lambda_{F_{i,j},T} & -\lambda_{F_{i,j},T} \\ -\lambda_{F_{i,j},T} & \lambda_{F_{i,j},T} \end{pmatrix}, \tag{16}$$

in matrix $\mathbf{M}$*, and the result remains a M-matrix with diagonal dominance in rows.* □

Similar theorem can be stated for monotone (non-negativity preserving) nonlinear TPFA scheme.

Theorem 2.2. *Let monotone (non-negativity preserving) nonlinear TPFA scheme is used for inter-cell Darcy flux discretization. Then the monotone EDFM from sections 1.1–1.4 with Darcy fluxes* (3)–(4) *is also monotone.*

Proof. The proof is identical to the previous theorem with the diagonal dominance in columns being used instead of dominance in rows. □

3 Conclusion

We present the monotone embedded discrete fracture method (mEDFM) for flows in fractured media. The method combines the EDFM approach with two nonlinear schemes: monotone nonlinear two-point flux approximation and compact nonlinear multi-point scheme satisfying the discrete maximum principle. The mEDFM method is extremum-preserving for the matrix-fracture system when combined with the extremum-preserving nonlinear FV scheme for matrix flow.

References

[1] I. Aavatsmark, G. Eigestad, B. Mallison, and J. Nordbotten. A compact multipoint flux approximation method with improved robustness. *Num. Meth. for Part. Diff. Eqs.*, 24(5):1329–1360, 2008.

[2] A. Chernyshenko and Y. Vassilevski. A finite volume scheme with the discrete maximum principle for diffusion equations on polyhedral meshes. In *Finite Volumes for Complex Applications VII-Methods and Theoretical Aspects*, pages 197–205. Springer, 2014.

[3] A. A. Danilov and Y. V. Vassilevski. A monotone nonlinear finite volume method for diffusion equations on conformal polyhedral meshes. *Russ. J. Numer. Anal. Math. Model.*, 24(3):207–227, 2009.

[4] H. Hajibeygi, D. Karvounis, and P. Jenny. A hierarchical fracture model for the iterative multiscale finite volume method. *J. Comput. Phys.*, 230:8729–8743, 2011.

[5] L. Li and S. H. Lee. Efficient Field-Scale Simulation of Black Oil in a Naturally Fractured Reservoir Through Discrete Fracture Networks and Homogenized Media. *SPE Reserv. Eval. Eng.*, 11:750–758, 2008.

[6] A. Moinfar, A. Varavei, K. Sepehrnoori, and R. T. Johns. Development of a Coupled Dual Continuum and Discrete Fracture Model for the Simulation of Unconventional Reservoirs. In *SPE Reserv. Simul. Symp.*, 2013.

[7] M. Tene, S. B. Bosma, M. S. Al Kobaisi, and H. Hajibeygi. Projection-based Embedded Discrete Fracture Model (pEDFM). *Adv. Water Resour.*, 105:205–216, 2017.

[8] K. M. Terekhov, B. T. Mallison, and H. A. Tchelepi. Cell-centered nonlinear finite-volume methods for the heterogeneous anisotropic diffusion problem. *J. Comput. Phys.*, 2017.